Modeling and Traversal of Pliable Materials for Tracked Robot Navigation

Camilo Ordonez[a], Ryan Alicea[a], Brandon Rothrock[b], Kyle Ladyko[a], Mario Harper[a], Sisir Karumanchi[b], Larry Matthies[b], and Emmanuel Collins[a]

[a]Center for Intelligent Systems, Control and Robotics (CISCOR) and the Department of Mechanical Engineering, Florida A&M University-Florida State University, Tallahassee,USA
[b]Jet Propulsion Laboratory, Pasadena, USA

ABSTRACT

In order to fully exploit robot motion capabilities in complex environments, robots need to reason about obstacles in a non-binary fashion. In this paper, we focus on the modeling and characterization of pliable materials such as tall vegetation. These materials are of interest because they are pervasive in the real world, requiring the robotic vehicle to determine when to traverse or avoid them. This paper develops and experimentally verifies a template model for vegetation stems. In addition, it presents a methodology to generate predictions of the associated energetic cost incurred by a tracked mobile robot when traversing a vegetation patch of variable density.

Keywords: Offroad Navigation, Vegetation Traversal, Tracked Robots

1. INTRODUCTION

Robots operating in the field are very likely to encounter terrains with vegetation that is taller than or of comparable height to the vehicle hull (hereafter referred to as tall vegetation. See Fig. 1). These environments are pervasive across the planet and occur during all seasons.

For simplicity and safety purposes robots to date tend to utilize a conservative approach that classifies such vegetated terrains as obstacles and then plans routes that navigate around them. For example, dense point clouds obtained using ladar data were used to segregate the environment into classes representing whether the terrain was traversable or non-traversable.[1] Also, the spaces between foliage have been used as the workspace within which paths could be generated.[2]

Figure 1. The RoMan tracked platform.

In relevant work on identification of vegetated terrain, a multispectral sensor was created out of a near-infrared and a visible light video camera,[3] leading to a robust chlorophyll detector in natural environments. Additional work focused on segmentation of ladar data into three classes using local three-dimensional point

Further author information: (Send correspondence to C. Ordonez)
E-mail: cordonez@fsu.edu

cloud statistics.[4,5] The classes are: 1) scatter to represent porous volumes such as grass and tree canopy, 2) linear to capture thin objects like wires or tree branches, and 3) surface to capture solid objects like ground surface, rocks, or large trunks. A perception methodology more geared towards vegetation traversal has also been developed.[6] In that research a combination of ladar and radar was employed to detect large tree trunks that can be occluded behind thick foliage.

A 3D algorithm to detect and classify obstacles has been proposed.[7] The approach classifies the obstacles as belonging to different obstacle types (rocks, vegetation, etc). It also included a terrain load bearing model, which was coupled with a suspension model of the vehicle to generate estimates of safe traversal speeds for the different terrains. Vegetation traversal has been studied,[8] where uniform patches of vegetation were characterized using a lumped frictional model. The developed terrain models were then used to plan trajectories that exploited the vehicle momentum to traverse the vegetation patches while avoiding vehicle immobilization.

Here we propose a methodology that models vegetated terrain as a set of stems of a given rotational stiffness and damping characteristics. The approach uses the developed stem models in conjunction with forward simulations of the robot to generate predictions of the energy required to traverse a given path. By doing this, robots can make informed decisions to decide if and how the terrain should be traversed.

The remainder of the paper is structured as follows: Section 2 discusses the template model developed to characterize pliable vegetation and also details a dynamic model to capture the interaction of the vehicle with a patch of vegetation. Section 3 presents simulation results of vegetation traversal and develops an estimation approach for the terrain model parameters. Finally, Section 4 contains concluding remarks and directions for future work.

2. MODELING

In this work, modeling is performed at two different scales. At a lower scale, single vegetation stems are modeled as thin rods anchored in the ground. Then, this template is extended to multiple stems and is combined with a model of the vehicle longitudinal dynamics.

2.1 Modeling of Pliable Vegetation

As illustrated in Fig. 2, vegetation is modeled locally as a thin rod anchored on the ground, with rotational stiffness k, and rotational damping b. The second order linear differential equation describing the dynamics of the stem can be expressed by

$$J\ddot{\theta} + b\dot{\theta} + k\theta = 0, \tag{1}$$

where J is the stem's moment of inertia, θ is the angle of the stem, and $\dot{\theta}$ and $\ddot{\theta}$ are its angular velocity and acceleration.

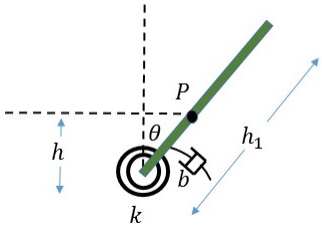

Figure 2. Model of a vegetation stem of length h_1, rotational stiffness k and rotational damping b. Here, h represents the location at which an external force F interacts with the stem.

To validate the model (1) a series of experiments where conducted on real vegetation as depicted in Figs. 3 through 5. During these experiments the vegetation stems were manually displaced from the vertical position to an angle $\theta(0) = \theta_0$ with zero initial velocity $\dot{\theta}(0) = 0$. Once the stem was released, its angular motion was tracked with a high speed camera. The moment of inertia was computed as $J = \frac{1}{3}mh_1^2$, where m is the mass of the stem and h_1 its length. The high speed data was then employed in conjunction with (1) to estimate k and b. Figures 3 through 5 show the good correspondence between the experimental data and the estimated models.

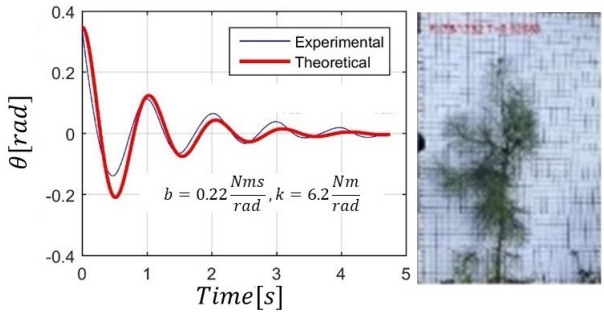

Figure 3. Estimation of stem model parameters for a medium size pine.

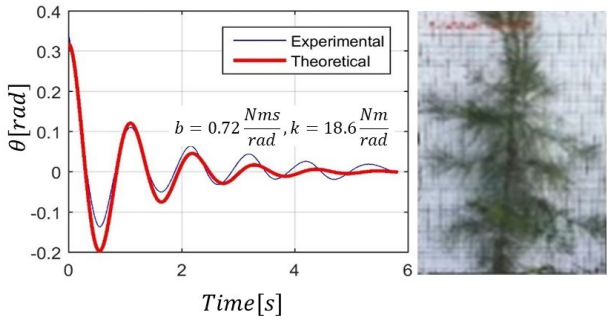

Figure 4. Estimation of stem model parameters for a large size pine.

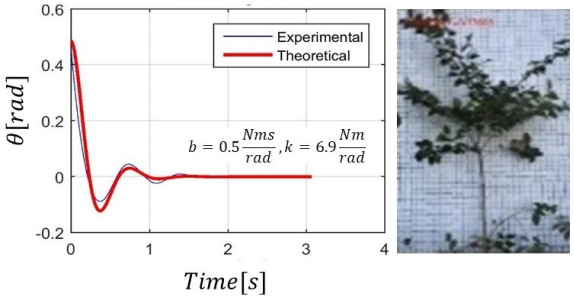

Figure 5. Estimation of stem model parameters for a shrub.

2.2 Modeling of Robot Longitudinal Dynamics while Traversing Tall Vegetation

Following Fig. 6, the robot longitudinal dynamics can be expressed as

$$M\ddot{x} + D(x, \dot{x}) + R_{res} = F, \tag{2}$$

where M is the robot's mass and F is the tractive force exerted by the robot tracks on the terrain. This force is required to accelerate the vehicle and to overcome the rolling resistance R_{res} and the drag D generated by the tall vegetation. Here, we assume that the terrain underneath the vegetation has the same properties as non-vegetated terrain in its proximity.

Referring back to Fig. 2, assuming a very small stem inertia J, and given that the robot bumper makes contact with the stem at a height h, one can convert the stem resistance torque $(b\dot{\theta} + k\theta)$ into a longitudinal and a perpendicular force acting at point P. The longitudinal force corresponds to the drag and is given by

$$D = \frac{1}{h}k\theta\cos^2\theta + \frac{1}{h}b\dot{\theta}\cos^2\theta, \tag{3}$$

which, as shown in Fig. 7, can be generalized to n stems. The overall drag force becomes

$$D = \frac{1}{h}\sum_{i=1}^{n}\alpha_i k_i\theta_i\cos^2\theta_i + \frac{1}{h}\sum_{i=1}^{n}\alpha_i b_i\dot{\theta}_i\cos^2\theta_i, \tag{4}$$

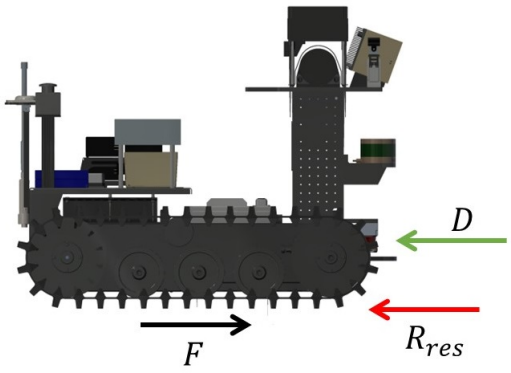

Figure 6. Longitudinal dynamic model. The force F is the tractive force, R_{res} is the rolling resistance and D is the drag force experienced due to the vegetation.

where $\alpha_i = 1$ if stem i is in contact with the vehicle, and 0 otherwise.

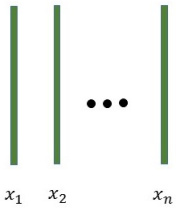

Figure 7. Multiple stems anchored at locations x_i.

3. SIMULATION RESULTS

Two important problems can be addressed in simulation. First, given vehicle commands and terrain properties, forward simulations through a patch can be conducted to estimate the energy needed to traverse a given path. Second, it is possible to study the problem of estimation of the stem's physical parameters (k and b) given simulated proprioceptive data.

3.1 Traversability Analysis

To perform traversability predictions, it is assumed that the vehicle is being commanded at a linear velocity v_d. Vehicle forward simulations must take into account the speed controller being employed by the vehicle, perceptual features of the terrain such as average height of the stems, patch length, stem density (i.e., number of stems per unit length), and stem physical properties (rotational stiffness and rotational damping). Once the drag on the vehicle is derived, the expected vehicle velocity profile and expected mechanical energy can be computed. To illustrate this, the scenario of Fig. 8 was considered. In this scenario the vehicle was commanded to move at a desired speed of $0.2m/s$. The simulations were run employing a PI controller that regulates the vehicle speed. The average vegetation height was $0.75m$, all stems were assumed of the same average rotational stiffness $k = 20\frac{Nm}{rad}$ and rotational damping $b = 0.22\frac{Nms}{rad}$. The patch length was $0.3m$, the rolling resistance was $0.5N$, and the vegetation stem density was of $13\frac{stems}{meter}$.

Using (4), it is possible to compute the drag on the vehicle at each instant during its motion. Once the drag D is obtained, the total tractive force F can be computed via (2). The instantaneous mechanical power is then given by $P = Fv$, where v is the current vehicle velocity. Finally, the expected mechanical energy required to traverse the patch can be estimated as $E = \int_0^t P dt$. Figures 9 and 10 show the results from the forward simulation corresponding to the scenario depicted in Fig. 8.

The second scenario shown in Fig. 11 depicts a more realistic field situation in which the vehicle encounters a vegetation patch of variable stem density. In order to select which path to take through the patch, a sound

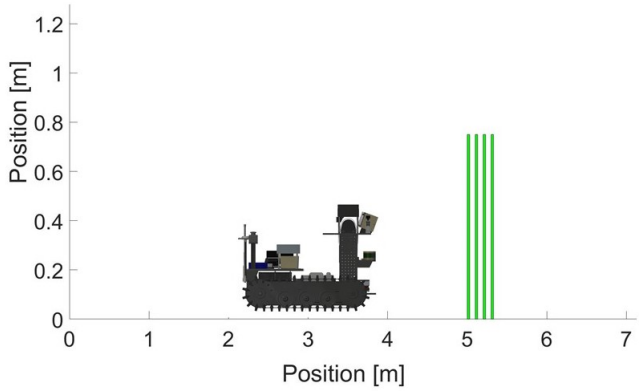

Figure 8. Scenario for forward simulations of vegetation traversal. The Vegetation patch has a density of $13\frac{stems}{meter}$.

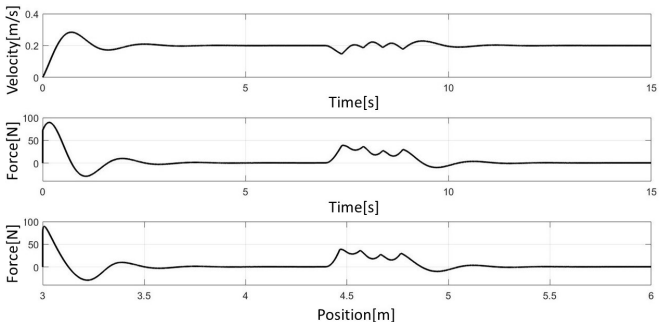

Figure 9. Velocity and tractive force profiles when the vehicle traverses the tall vegetation patch of Fig. 8.

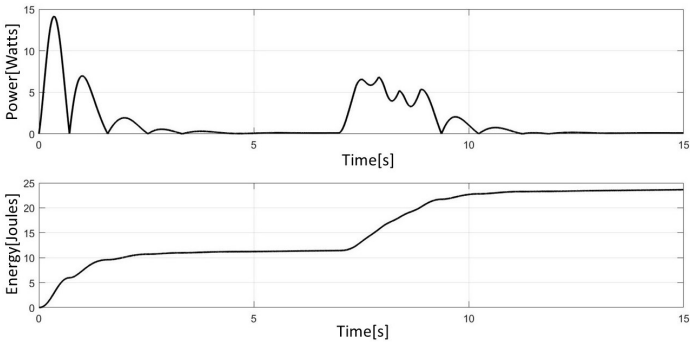

Figure 10. Power and energy profiles when the vehicle traverses the tall vegetation patch of Fig. 8.

strategy consists in estimating the energetic cost of traversal at different possible entry points to the patch. The test entry points are here chosen uniformly distributed along the Y-axis at an interval of $0.2m$, and assumed that the vehicle moves parallel to the X-axis and that motion outside the patch requires negligible energy.

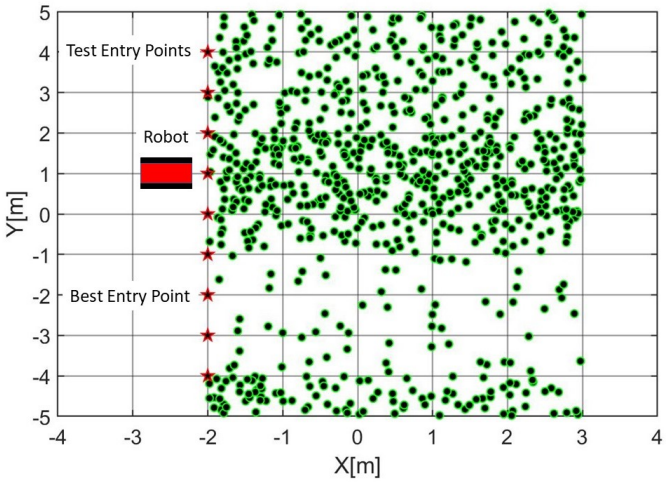

Figure 11. Vegetation patch of variable density. The robot is faced with multiple entry points to the patch. For ease of visualization only a few entry points are displayed. However, in simulation they were uniformly distributed along the Y-axis every $0.2m$.

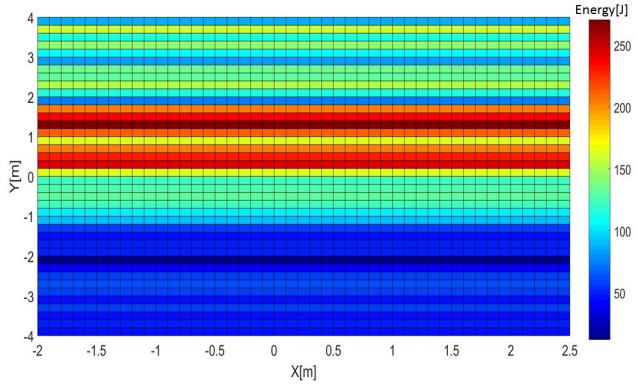

Figure 12. Energetic cost predictions for the different entry points. The discretization along Y corresponds to entry point candidates (every $0.2m$). The colors in this plot represent the total energy required to traverse the patch with the vehicle center line at the corresponding entry point. In this scenario, the entry point at $(-2, -2)$ in Fig. 11 has the lowest cost.

Figure 12, shows the energetic cost incurred by selecting the respective entry point. In this scenario, the vehicle should choose the entry point at $(-2, -2)$, which has the lowest energetic cost. Note that the figure colors represent total energy consumed by the vehicle when traversing the patch from the entry point until the end of the patch.

3.2 Parameter Estimation

The second problem of interest addressed here in simulation is a parameter estimation problem. That is, given observations of the robot velocity, tractive force, and knowledge of perceptual features such as average stem height, patch length, and stem density, perform estimation of the stem parameters k and b.

The rolling resistance is estimated as the average tractive force exerted by the robot when is moving at a steady state velocity and is not in contact with the vegetation. From (2) the measured drag force at time j becomes $D_j = F_j - M\ddot{x}_j - R_{res}$. As the robot moves over the terrain, (4) can be used to generate a prediction

of the expected drag at the same time instant. Following this process for P observations, we can write in matrix form

$$D = Hq + \epsilon, \tag{5}$$

where

$$D = \begin{bmatrix} D_1 \\ D_2 \\ \vdots \\ D_p \end{bmatrix}, \quad q = \begin{bmatrix} k \\ b \end{bmatrix},$$

and

$$H = \begin{bmatrix} \sum_{i=1}^{n} \frac{\alpha_{i1}}{h} \theta_{i1} \cos^2 \theta_{i1} & \sum_{i=1}^{n} \frac{\alpha_{i1}}{h} \dot{\theta}_{i2} \cos^2 \theta_{i1} \\ \sum_{i=1}^{n} \frac{\alpha_{i2}}{h} \theta_{i1} \cos^2 \theta_{i2} & \sum_{i=1}^{n} \frac{\alpha_{i2}}{h} \dot{\theta}_{i2} \cos^2 \theta_{i2} \\ \vdots & \vdots \\ \sum_{i=1}^{n} \frac{\alpha_{ip}}{h} \theta_{ip} \cos^2 \theta_{ip} & \sum_{i=1}^{n} \frac{\alpha_{ip}}{h} \dot{\theta}_{ip} \cos^2 \theta_{ip} \end{bmatrix}, \tag{6}$$

where ϵ represent the error in the drag prediction. Since (5) is an overdetermined system, q is estimated as the least squares solution,

$$\hat{q} = (H^T H)^{-1} H^T D. \tag{7}$$

To test the estimation formulation, two forward simulations over the scenario shown in Fig. 8 were performed at $0.2m/s$ and at $0.5m/s$. The data from both simulations was stacked and casted in matrix form using (5). The actual parameters of the vegetation were $R_{res} = 0.5N$, $k = 20\frac{Nm}{rad}$, and $b = 0.22\frac{Nms}{rad}$.

The estimation results are heavily dependent on the closed-loop velocity controller and the sampling rate of the low level data. Table 1 shows identification results for different sampling rates. The second column of Table 1 denotes if a closed-loop speed controllers was used in the simulation or whether perfect velocity tracking was assumed (i.e., no closed-loop speed control used). As expected, when perfect velocity tracking was assumed, the estimation results are in closer agreement with the actual vegetation parameters. However, perfect velocity tracking in these environments is unrealistic. From Table 1, it is possible to conclude that in realistic terrain traversal, the robotic platform will need to collect proprioceptive data (encoder and motor currents) at sampling frequencies that exceed $1kHz$.

Table 1. Parameter estimation results for different speed controllers and sampling rates.

Sampling Frequency $[kHz]$	Perfect Speed Tracking Assumed?	$\hat{k}$ $[\frac{Nm}{rad}]$	$\hat{b}$ $[\frac{Nms}{rad}]$	$\hat{R}_{res}$ $[N]$
5	No	20.010	0.215	0.499
5	Yes	20.004	0.219	0.500
1	No	20.050	0.196	0.500
1	Yes	20.018	0.217	0.500
0.1	No	20.429	-0.011	0.499
0.1	Yes	20.019	0.218	0.500

4. CONCLUSIONS AND FUTURE WORK

In this paper a stem model was proposed and experimentally validated. The developed model was then combined with the longitudinal dynamics of a tracked platform to develop estimates of energetic traversal costs over 2 dimensional patches of variable density. In addition, simulation results were conducted to estimate stem physical parameters provided simulated proprioceptive data.

The work here proposed will be experimentally validated on the RoMan platform depicted in Fig. 1. Additional work will concentrate on studying perception mechanisms to automatically estimate stem density.

ACKNOWLEDGMENT

This work was supported by the collaborative participation in the Robotics Consortium sponsored by the U.S. Army Research Laboratory under the Collaborative Technology Alliance Program, Cooperative Agreement DAAD 19-01-2-0012. The U.S. Government is authorized to reproduce and distribute reprints for Government purposes not withstanding any copyright notation thereon.

REFERENCES

[1] Krüsi, P., Furgale, P., Bosse, M., and Siegwart, R., "Driving on point clouds: Motion planning, trajectory optimization, and terrain assessment in generic nonplanar environments," *Journal of Field Robotics* **34**(5), 940–984 (2017).

[2] Vandapel, N., Kuffner, J., and Amidi, O., "Planning 3-d path networks in unstructured environments," in [*Proceedings of the 2005 IEEE International Conference on Robotics and Automation*], 4624–4629 (April 2005).

[3] Bradley, D., Thayer, S., Stentz, A., and Rander, P., "Vegetation detection for mobile robot navigation," tech. rep. (2004).

[4] Hebert, M. and Vandapel, N., "terrain classification techniques from ladar data for autonomous navigation," in [*Collaborative Technology Alliances conference*], (May 2003).

[5] Lalonde, J.-F., Vandapel, N., Huber, D., and Hebert, M., "Natural terrain classification using three-dimensional ladar data for ground robot mobility," *Journal of Field Robotics* **23**, 839 – 861 (November 2006).

[6] Matthies, L., Bergh, C., Castano, A., Macedo, J., and Manduchi, R., "Obstacle detection in foliage with ladar and radar," in [*Proceedings of International Symposium of Robotics Research*], (2003).

[7] Talukder, A., Manduchi, R., Owens, K., Matthies, L., Castano, A., and Hogg, R., "Autonomous terrain characterization and modeling for dynamic control of unmanned vehicles," in [*IEEE/RSJ Conference on Intelligent Robots and Systems (IROS)*], (2002).

[8] Ordonez, C., Gupta, N., Chuy, O., and Collins, E., "Momentum based traversal of mobility challenges for autonomous ground vehicles," in [*Proceedings of the IEEE Conference on Robotics and Automation*], (May 2013).